Nigerian Research Journal of Engineering and Environmental Sciences 6(1) 2021 pp. 236-247

Nigerian Research Journal of Engineering and Environmental Sciences
Journal homepage: www.rjees.com

Original Research Article

On Approximate Solutions of a Fractional Chemotaxis-Haptotaxis Model via two Computational Schemes

***[1]Okposo, N.I., [2]Okposo, E.N. and [1]Ossaiugbo, M.I.**

[1]Department of Mathematics, Delta State University, Abraka, PMB 1, Abraka, Delta State, Nigeria.
[2]Department of Mathematics, College of Education, Agbor, PMB 2090, Agbor, Delta State, Nigeria.
*newstar4sure@gmail.com

ARTICLE INFORMATION

Article history:
Received 12 Feb, 2021
Revised 17 Apr, 2021
Accepted 20 Apr, 2021
Available online 30 Jun, 2021

Keywords:
Cancer-invasion
Chemotaxis-haptotaxis model
Caputo derivative
q-homotopy analysis transform method
Homotopy perturbation transform method

ABSTRACT

In this paper, the q-homotopy analysis transform method (q-HATM) and homotopy perturbation transform method (HPTM) were employed to obtain analytic series solutions for a coupled system of nonlinear time-fractional chemotaxis-haptotaxis model. The applied methods yielded solutions in the form of convergent series and does not involve discretization or linearization. Furthermore, the obtained analytical results were compared for both methods via graphical representations for distinct arbitrary order with a view to demonstrating the efficiency of the methods in handling even more complex nonlinear systems from mathematical biology.

1. INTRODUCTION

Over the past few decades, several tools from fractional calculus have been extensively used to model a wide variety of real-world problems in the form of fractional (or non-integer) order (ordinary or partial) differential or integral equations. In existing literature, the Riemann-Liouville and Caputo derivatives are the most commonly used fractional derivatives (Podlubny, 1999; Kilbas et al., 2006). One advantage of fractional mathematical models over their classical integer order counterparts is that essential information the present state and past states are taken into account in the mathematical formulation of physical problems. Thus, fractional calculus provides very suitably tools for modelling even more complex physical systems associated with memory dependent phenomena, hereditary properties, and non-local distributed behaviors (Podlubny, 1999; Kilbas et al., 2006).

Determining the exact solutions of fractional order differential equations is usually more complicated than obtaining same for their classical integer-order counterparts. Hence, in recent years, many authors have

shifted their interest towards developing effective and efficient analytical techniques for determining approximate solutions for this class of equations. Some of these well-established and powerful analytical techniques include the Adomian decomposition method (Adomian, 1988; Wazwaz and El-Sayed 2001), variational iteration method (He, 1997, 1998; Prakash et al., 2015; Prakash and Kumar, 2016a, 2016b), homotopy analysis method (HAM) (Liao, 1992, 1997), homotopy perturbation method (HPM) (He, 1999, 2003, 2006, Yildirim, 2009, 2010). Other efficient techniques such as the q −homotopy analysis transform method (q − HATM) (Singh, 2016; Prakasha et al., 2019; Veeresha et al., 2019; Newton and Abel, 2020) as well as the homotopy perturbation transform method (HPTM) (Khan, 2011; Tiwana et al., 2017) are modifications of existing methods. The q − HATM is a combination of the classical q −homotopy analysis method (q −HAM) (El-Tawil and El-Huseen, 2012) and the Laplace transform method (LTM) while the HPTM combines the classical HPM and the LTM. The q −HATM incorporates two auxiliary parameters $\hbar$ and n, which helps us to adjust and control the convergence of analytic solutions. Both methods simplify computational time and procedures compared with other traditional techniques while maintaining the great efficiency of the obtained results. Furthermore, they do not involve any form of discretization or linearization.

In this paper, two analytical techniques, namely, the q −homotopy analysis transform method (q −HATM) and the homotopy perturbation transform method (HPTM) were employed to obtain approximate series solutions for a coupled nonlinear system of time-fractional parabolic-parabolic-ODE given by Equation (1):

$$\begin{cases} {}_0^C D_\varsigma^\sigma u = d_u \frac{\partial^2 u}{\partial \zeta^2} - \chi \frac{\partial}{\partial x}\left(u \frac{\partial v}{\partial \zeta}\right) - \xi \frac{\partial}{\partial x}\left(u \frac{\partial w}{\partial \zeta}\right) + \mu u(1 - u - w), \\ {}_0^C D_\varsigma^\sigma v = d_v \frac{\partial^2 v}{\partial \zeta^2} - \beta v + \alpha u, \\ {}_0^C D_\varsigma^\sigma w = -\delta v w + \eta w(1 - u - w), \end{cases} \tag{1}$$

using the initial conditions in Equations (2):

$$u(\zeta, 0) = e^{-\varepsilon \zeta^2}, v(\zeta, 0) = M e^{-\varepsilon \zeta^2}, \; w(\zeta, 0) = 1 - M e^{-\varepsilon \zeta^2} \tag{2}$$

where $\varepsilon > 0$ and $M > 0$ are constants to be specified later. Here, the fractional differential operator is of the Caputo type. Clearly, when $\sigma = 1$, then the coupled system of fractional differential Equations (1) which incorporate non-locality features reduces to the classical integer-order chemotaxis-haptotaxis model given by Equation (3):

$$\begin{cases} D_\varsigma u = d_u \frac{\partial^2 u}{\partial \zeta^2} - \chi \frac{\partial}{\partial \zeta}\left(u \frac{\partial v}{\partial \zeta}\right) - \xi \frac{\partial}{\partial \zeta}\left(u \frac{\partial w}{\partial \zeta}\right) + \mu u(1 - u - w), \\ D_\varsigma u = d_v \frac{\partial^2 v}{\partial \zeta^2} - \beta v + \alpha u, \\ D_\varsigma u = -\delta v w + \eta w(1 - u - w). \end{cases} \tag{3}$$

The coupled system of Equations (3), also known as cancer invasion model, was proposed by Chaplain and Lolas (2006) to describe the interaction between the cancer cells, matrix degrading enzymes (MDEs) and healthy tissues or extracellular matrix (ECM). Here, $u = u(\zeta, \varsigma)$ denotes the cancer cell density, $v = v(\zeta, \varsigma)$ denotes the concentration of MDEs and $w = w(\zeta, \varsigma)$ denotes the ECM density. The first parabolic expression of Equation (3) describes the time evolution of the cancer cells where d_u represents the random motility coefficient of cancer cells and μ is the proliferation rate of the cells. This equation also incorporates two very important cell migration features, namely, chemotaxis and haptotaxis represented by the terms $\chi \frac{\partial}{\partial \zeta}\left(u \frac{\partial v}{\partial \zeta}\right)$ and $\xi \frac{\partial}{\partial \zeta}\left(u \frac{\partial w}{\partial \zeta}\right)$, respectively, where $\chi > 0$ and $\xi > 0$ are chemotactic and haptotactic sensitivity constants, respectively. Chemotaxis means the directed movement of cancer cells in response to the concentration gradient of a chemical substance. Usually, the cells sense the chemical secreted and move toward lower concentrations of this chemical substance until they reach the site of secretion. However, the solution may lack gradient and instead, non-diffusible adhesive molecules could be present in increasing

amount within the components of the ECM. Consequently, since the cells have to adhere to the ECM fibers in order to move, they will migrate from a region where the concentration of existing adhesive molecule is high to an area with a lower concentration. This type of movement is called haptotaxis. The MDE concentration is described by the second parabolic expression of Equation (3) where d_v, β and α are positive constants having biological importance. The MDE is produced by the cancer cells, it is assumed to diffuse throughout the ECM and then decay. Furthermore, since the ECM is static, the effect of diffusion can be neglected so that we only consider its degradation by MDEs upon contact. Apart from competing for space with cancer cells, it is also assumed that in the absence of cancer cells, the ECM is capable of remodeling back to a healthy level, leading to the third expression of Equation (3) for the time evolution of the ECM, with some positive degradation rate δ and remodeling rate η. For other variant cancer invasion models can be found in the following references (Gatenby and Gawlinski, 1996; Berry and Larreta-Graade, 1999; Sachs et al. 2001; McAneney and O'Rourke. 2007; Lin et al. 2012; Markl et al. 2013). Furthermore, Anderson et al. (2000) presented a detailed discussion on the complex multistep processes of cancer invasion and metastasis.

2. MATERIALS AND METHODS

2.1. Preliminary Tools from Fractional Calculus

In this section some useful tools from the theory of fractional calculus are briefly introduced. In the sequel, the usual Euler's gamma function is denoted by $\Gamma(\cdot)$ and for $r \in \mathbb{N}$, $D_{\varsigma}^{r} f(\varsigma) = \frac{d^r}{d\varsigma^r} f(\varsigma) = f^{(r)}(\varsigma)$ denotes the rth-order ordinary derivative of the function f with respect to ς. Furthermore, we state the following definitions:

Definition 1: Let $f(\varsigma)$, $\varsigma > 0$ be a real function in the space $C_{\mu}(\mu \in \mathbb{R})$ if there exists a real number $p(> \mu)$ such that $f(\varsigma) = \zeta^{p} f_1(\varsigma)$, where $f_1(\varsigma) \in C[0, \infty)$, and it is said to be in C_{μ}^{r} if $f^{(r)} \in C_{\mu}$ (Podlubny, 1999).

Definition 2: The Riemann-Liouville integral of order σ of a function $f \in C_{\mu}$, $\mu \geq -1$ is defined by (Podlubny, 1999; Kilbas et al., 2006):

$$I_t^{\sigma} f(\varsigma) = \begin{cases} \frac{1}{\Gamma(\sigma)} \int_0^t (\varsigma - \theta)^{\sigma-1} f(\theta) d\theta \ , & \sigma > 0, t > 0, \\ f(\varsigma), & \sigma = 0, t > 0. \end{cases} \tag{4}$$

Definition 3: Let $\sigma > 0$. The Riemann-Liouville fractional derivative of a function $f \in C_{-1}^{r}$ $(r \in \mathbb{Z}^{+})$ is defined as (Podlubny, 1999; Kilbas et al., 2006):

$${}_0^{RL}D_{\varsigma}^{\sigma} f(\varsigma) = \begin{cases} D_t^r f(\varsigma), & \sigma = r \in \mathbb{N}, \\ \frac{1}{\Gamma(r-\sigma)} D_t^r \left[\int_0^t (\varsigma - \theta)^{r-\sigma-1} f(\theta) d\theta \right], & r - 1 < \sigma < r \in \mathbb{N}. \end{cases} \tag{5}$$

Definition 4: Let $\sigma > 0$. The fractional derivative of a function $f \in C_{-1}^{r}$ in the Caputo sense is defined as (Podlubny, 1999; Kilbas et al., 2006):

$${}_0^{C}D_{\varsigma}^{\sigma} f(\varsigma) = \begin{cases} \dfrac{d^r f(\varsigma)}{dt^r}, & \sigma = r \in \mathbb{N}, \\ \dfrac{1}{\Gamma(r-\sigma)} \displaystyle\int_0^t (\varsigma - \theta)^{r-\sigma-1} f(\theta) d\theta, & m - 1 < \sigma < r \in \mathbb{N}. \end{cases} \tag{6}$$

Definition 5: The Laplace transform associated with the Caputo fractional derivative of a function $f \in C_{-1}^{r}$ is defined as (Podlubny, 1999; Kilbas et al., 2006):

$$\mathcal{L}[{}_0^{C}D_t^{\sigma} f(\varsigma)] = s^{\sigma} \mathcal{L}[f(\varsigma)] - \sum_{k=0}^{r-1} s^{\sigma-k-1} f^{(k)}(0^{+}) \ , \ r - 1 < \sigma \leq r \tag{7}$$

where $\mathcal{L}$ represents the Laplace transform operator.

2.2. q −HATM Series Solution for the Time-Fractional Model

In the present section, the q-HATM (see Prakash et al., 2019; Newton and Abel, 2020, for the basic procedure and convergence analysis of the method) is applied to obtain approximate series solutions for the time fractional chemotaxis-haptotaxis model Equations 1-2. As a first step in applying the q-HATM, we operate either sides of each equation in (Equation 1) with the Laplace transform operator and use the initial data (Equation 2) together with the Laplace transform property for the Caputo derivative (Equation 7) to obtain the following system of equations after some simplifications.

$$\begin{cases} \mathcal{L}[u(\zeta,\varsigma)] - \frac{e^{-\varepsilon\zeta^2}}{s} \\ \qquad -\frac{1}{s^{\sigma}}\,\mathcal{L}\left[d_u\,\frac{\partial^2 u}{\partial\zeta^2} - \chi\,\frac{\partial}{\partial\zeta}\left(u\,\frac{\partial v}{\partial\zeta}\right) - \xi\,\frac{\partial}{\partial\zeta}\left(u\,\frac{\partial w}{\partial\zeta}\right) + \mu u(1-u-w)\right] = 0, \\ \mathcal{L}[v(\zeta,\varsigma)] - \frac{Me^{-\varepsilon\zeta^2}}{s} - \frac{1}{s^{\sigma}}\,\mathcal{L}\left[d_v\,\frac{\partial^2 u}{\partial\zeta^2} - \beta v + \alpha u\right] = 0, \\ \mathcal{L}[w(\zeta,\varsigma)] - \frac{1-Me^{-\varepsilon\zeta^2}}{s} - \frac{1}{s^{\sigma}}\,\mathcal{L}[-\delta vw + \eta w(1-u-w)] = 0. \end{cases} \tag{8}$$

In view of the classical HAM, the system of nonlinear operators given in (Equation 9) were constructed for the real-valued functions $\Theta_1(\zeta,\varsigma;\,q)$, $\Theta_2(\zeta,\varsigma;\,q)$, $\Theta_3(\zeta,\varsigma;\,q)$.

$$\begin{cases} \mathcal{N}_1[\Theta_1(\zeta,\varsigma;\,q)] = \mathcal{L}[\Theta_1(\zeta,\varsigma;\,q)] - \frac{e^{-\varepsilon\zeta^2}}{s} \\ \qquad -\frac{1}{s^{\sigma}}\,\mathcal{L}\left[d_u\,\frac{\partial^2\Theta_1(\zeta,\varsigma;\,q)}{\partial\zeta^2} - \chi\,\frac{\partial}{\partial\zeta}\left(\Theta_1(\zeta,\varsigma;\,q)\frac{\partial\Theta_2(\zeta,\varsigma;\,q)}{\partial\zeta}\right)\right. \\ \qquad \left. -\xi\,\frac{\partial}{\partial x}\left(\Theta_1(\zeta,\varsigma;\,q)\frac{\partial w}{\partial\zeta}\right) + \mu\Theta_1(\zeta,\varsigma;\,q)\big(1-\Theta_1(\zeta,\varsigma;\,q)-\Theta_3(\zeta,\varsigma;\,q)\big)\right], \\ \mathcal{N}_2\big[\,\Theta_2\big((\zeta,\varsigma;\,q);\,q\big)\big] = \mathcal{L}[\Theta_2(\zeta,\varsigma;\,q)] - \frac{Me^{-\varepsilon\zeta^2}}{s} \\ \qquad -\frac{1}{s^{\sigma}}\,\mathcal{L}\left[d_v\,\frac{\partial^2\Theta_2(\zeta,\varsigma;\,q)}{\partial\zeta^2} - \beta\Theta_2(\zeta,\varsigma;\,q) + \alpha\Theta_1(\zeta,\varsigma;\,q)\right], \\ \mathcal{N}_3[\,\Theta_3(\zeta,\varsigma;\,q)] = \mathcal{L}[\Theta_3(\zeta,\varsigma;\,q)] - \frac{1-Me^{-\varepsilon\zeta^2}}{s} - \frac{1}{s^{\sigma}}\,\mathcal{L}[-\delta\Theta_2(\zeta,\varsigma;\,q)\Theta_3(\zeta,\varsigma;\,q) \\ \qquad +\eta\Theta_3(\zeta,\varsigma;\,q)\big(1-\Theta_1(\zeta,\varsigma;\,q)-\Theta_3(\zeta,\varsigma;\,q)\big)]. \end{cases} \tag{9}$$

where $q \in \left[0,\ \frac{1}{n}\right]$, $(n \geq 1)$ denotes the embedding parameter. Furthermore, the following zeroth-order deformation equations are constructed according to the HAM (Liao, 1992, 1997):

$$\begin{aligned} (1-nq)\mathcal{L}[\Theta_1(\zeta,\varsigma;\,q) - u_0(\zeta,\varsigma)] &= \hbar q\mathcal{N}[\Theta_1(\zeta,\varsigma;\,q)] \\ (1-nq)\mathcal{L}[\Theta_2(\zeta,\varsigma;\,q) - v_0(\zeta,\varsigma)] &= \hbar q\mathcal{N}[\Theta_2(\zeta,\varsigma;\,q)] \\ (1-nq)\mathcal{L}[\Theta_3(\zeta,\varsigma;\,q) - w_0(\zeta,\varsigma)] &= \hbar q\mathcal{N}[\Theta_3(\zeta,\varsigma;\,q)] \end{aligned} \tag{10}$$

where $\hbar \neq 1$ is an auxiliary parameter and $u_0(\zeta,\varsigma)$, $v_0(\zeta,\varsigma)$, $w_0(\zeta,\varsigma)$ are initial guesses of and $u(\zeta,\varsigma)$, $v(\zeta,\varsigma)$, $w(\zeta,\varsigma)$ respectively. Clearly, the following equations hold true:

$$\begin{cases} \Theta_1(\zeta,\varsigma;\,0) = u_0(\zeta,\varsigma) \ \ if\ q=0 \ \text{and} \ \ \Theta_1\left(\zeta,\varsigma;\,\frac{1}{n}\right) = u(\zeta,\varsigma) \ \ \text{if} \ q=\frac{1}{n}, \\ \Theta_2(\zeta,\varsigma;\,0) = v_0(\zeta,\varsigma) \ \ if\ q=0 \ \text{and} \ \ \Theta_2\left(\zeta,\varsigma;\,\frac{1}{n}\right) = v(\zeta,\varsigma) \ \ \text{if} \ q=\frac{1}{n}, \\ \Theta_3(\zeta,\varsigma;\,0) = u_0(\zeta,\varsigma) \ \ if\ q=0 \ \text{and} \ \ \Theta_3\left(\zeta,\varsigma;\,\frac{1}{n}\right) = w(\zeta,\varsigma) \ \ \text{if} \ q=\frac{1}{n}. \end{cases} \tag{11}$$

This implies that by varying q from 0 to $\frac{1}{n}$, the functions $\Theta_1(\zeta,\varsigma;\,q), \Theta_2(\zeta,\varsigma;\,q), \Theta_3(\zeta,\varsigma;\,q)$ transit from the initial functions $u_0(\zeta,\varsigma)$, $v_0(\zeta,\varsigma)$, $w_0(\zeta,\varsigma)$ to the solutions $u(\zeta,\varsigma)$, $v(\zeta,\varsigma)$, $w(\zeta,\varsigma)$, respectively. Thus, the set of deformation equations of mth order are expressed as:

$$\begin{aligned}
&\mathcal{L}[u_r(\zeta,\varsigma) - \aleph_r u_{r-1}(\zeta,\varsigma)] = \hbar R_{u,r}[\vec{u}_{r-1}],\\
&\mathcal{L}[v_r(\zeta,\varsigma) - \aleph_r v_{r-1}(\zeta,\varsigma)] = \hbar R_{v,r}[\vec{v}_{r-1}],\\
&\mathcal{L}[w_r(\zeta,\varsigma) - \aleph_r w_{r-1}(\zeta,\varsigma)] = \hbar R_{w,r}[\vec{w}_{r-1}],
\end{aligned} \tag{12}$$

where

$$\aleph_r = \begin{cases} 0, & r \le 1, \\ n, & r > 1, \end{cases}$$

and

$$\begin{cases}
R_{u,r}[\vec{u}_{r-1}] = \mathcal{L}[u_r(\zeta,\varsigma)] - \left(1 - \dfrac{\aleph_r}{n}\right)\left(\dfrac{e^{-\varepsilon\zeta^2}}{s}\right) \\
\qquad -\dfrac{1}{s^{\sigma}}\,\mathcal{L}\left[d_u\,\dfrac{\partial^2 u_{r-1}}{\partial\zeta^2} - \chi\sum_{i=0}^{r-1}\dfrac{\partial}{\partial\zeta}\left(u_i\,\dfrac{\partial v_{r-1-i}}{\partial\zeta}\right) - \xi\sum_{i=0}^{r-1}\dfrac{\partial}{\partial\zeta}\left(u_i\,\dfrac{\partial w_{r-1-i}}{\partial\zeta}\right)\right] \\
\qquad +\mu\left(u_{m-1} - \sum_{i=0}^{r-1} u_i u_{r-1-i} - \sum_{i=0}^{r-1} u_i w_{r-1-i}\right), \\
R_{v,r}[\vec{v}_{r-1}] = \mathcal{L}[v_r(\zeta,\varsigma)] - \left(1 - \dfrac{\aleph_r}{n}\right)\left(\dfrac{Me^{-\varepsilon\zeta^2}}{s}\right) \\
\qquad -\dfrac{1}{s^{\sigma}}\,\mathcal{L}\left[d_v\,\dfrac{\partial^2 v_{r-1}}{\partial\zeta^2} - \beta v_{r-1} + \lambda u_{r-1}\right] \\
R_{w,r}[\vec{w}_{r-1}] = \mathcal{L}[w_r(\zeta,\varsigma)] - \left(1 - \dfrac{\aleph_r}{n}\right)\left(\dfrac{1 - Me^{-\varepsilon\zeta^2}}{s}\right) \\
\qquad -\dfrac{1}{s^{\sigma}}\,\mathcal{L}\left[-\delta\sum_{i=0}^{r-1} v_i w_{r-1-i} + \eta\left(w_{r-1} - \sum_{i=o}^{r-1} w_i w_{r-1-i} - \sum_{i=0}^{r-1} w_i u_{r-1-i}\right)\right].
\end{cases} \tag{13}$$

Substituting (Equations 13) into (Equations 12) and operating the resulting set of equations with the inverse Laplace transform $\mathcal{L}^{-1}$ yields the following set of recursive relations

$$\begin{cases}
u_r(x,t) = (\aleph_r + \hbar)u_{r-1} - \hbar\left(1 - \dfrac{\aleph_r}{n}\right)\mathcal{L}^{-1}\left(\dfrac{e^{-\varepsilon\zeta^2}}{s}\right) \\
\qquad -\hbar\mathcal{L}^{-1}\left\{\dfrac{1}{s^{\sigma}}\,\mathcal{L}\left[d_u\,\dfrac{\partial^2 u_{r-1}}{\partial\zeta^2} - \chi\sum_{i=0}^{r-1}\dfrac{\partial}{\partial\zeta}\left(u_i\,\dfrac{\partial v_{r-1-i}}{\partial\zeta}\right) - \xi\sum_{i=0}^{r-1}\dfrac{\partial}{\partial\zeta}\left(u_i\,\dfrac{\partial w_{r-1-i}}{\partial\zeta}\right)\right]\right\} \\
\qquad -\mu\left(u_{r-1} - \sum_{i=0}^{r-1} u_i u_{r-1-i} - \sum_{i=0}^{r-1} u_i w_{r-1-i}\right), \\
v_r(x,t) = (\aleph_r + \hbar)v_{r-1} - \hbar\left(1 - \dfrac{\aleph_r}{n}\right)\mathcal{L}^{-1}\left(\dfrac{Me^{-\varepsilon\zeta^2}}{s}\right) \\
\qquad -\hbar\mathcal{L}^{-1}\left\{\dfrac{1}{s^{\sigma}}\,\mathcal{L}\left[d_v\,\dfrac{\partial^2 v_{r-1}}{\partial\zeta^2} - \beta v_{r-1} + \lambda u_{r-1}\right]\right\}, \\
w_r(x,t) = \aleph_r w_{r-1} - \hbar\left(1 - \dfrac{\aleph_r}{n}\right)\mathcal{L}^{-1}\left(\dfrac{1 - Me^{-\varepsilon\zeta^2}}{s}\right) \\
\qquad -\hbar\mathcal{L}^{-1}\left\{\dfrac{1}{s^{\sigma}}\,\mathcal{L}\left[-\delta\sum_{i=0}^{r-1} v_i w_{r-1-i} + \eta\left(w_{r-1} - \sum_{i=o}^{r-1} w_i w_{r-1-i} - \sum_{i=0}^{r-1} w_i u_{r-1-i}\right)\right]\right\}.
\end{cases} \tag{14}$$

Taking $\mu = \eta = 0$ in (Equation 14) for the sake of computational simplicity, we obtain the following few q −HATM solution iterations for the fractional model (Equations 1 to 2):

$$\begin{cases} u_0(\zeta,\varsigma) = \mathrm{e}^{-\varepsilon\zeta^2}, \quad v_0(\zeta,\varsigma) = M\mathrm{e}^{-\varepsilon\zeta^2}, \quad w_0(\zeta,\varsigma) = 1 - M\mathrm{e}^{-\varepsilon\zeta^2} \\ u_1(\zeta,\varsigma) = -\dfrac{2\hbar\varepsilon\mathrm{e}^{-\varepsilon\zeta^2}\left(\mathrm{e}^{-\varepsilon\zeta^2}\left(-4\zeta^2\varepsilon+1\right)(\chi-\xi)M + d_u\left(2\zeta^2\varepsilon-1\right)\right)\varsigma^{\sigma}}{\Gamma(\sigma+1)} \\ v_1(\zeta,\varsigma) = -\dfrac{\hbar\mathrm{e}^{-\varepsilon\zeta^2}\left(\lambda + \left(2\varepsilon d_v\left(2\zeta^2\varepsilon-1\right) - \beta\right)M\right)\varsigma^{\sigma}}{\Gamma(\sigma+1)} \\ w_1(\zeta,\varsigma) = -\dfrac{\hbar\delta\mathrm{e}^{-\varepsilon\zeta^2}M\left(M\mathrm{e}^{-\varepsilon\zeta^2}-1\right)\varsigma^{\sigma}}{\Gamma(\sigma+1)} \\ \quad . \\ \quad . \\ \quad . \end{cases} \tag{15}$$

Consequently, all q −HATM solution iterations for $\mathrm{r} \geq 2$ can be generated from (Equations 14) in the same manner. Finally, the q −HATM series solution to the time-fractional chemotaxis-haptotaxis model (Equations 1-2) is given by:

$$\begin{cases} u(\zeta,\varsigma) = u_0(\zeta,\varsigma) + \sum_{r=1}^{\infty} u_r(\zeta,\varsigma)\left(\frac{1}{n}\right)^r, \\ v(\zeta,\varsigma) = v_0(\zeta,\varsigma) + \sum_{r=1}^{\infty} v_r(\zeta,\varsigma)\left(\frac{1}{n}\right)^r, \\ w(\zeta,\varsigma) = w_0(\zeta,\varsigma) + \sum_{r=1}^{\infty} w_r(\zeta,\varsigma)\left(\frac{1}{n}\right)^r. \end{cases} \tag{16}$$

2.3. HPTM Series Solution for the Time-Fractional

Here, the HPTM (see Khan, 2011 and Tiwana et al., 2017, where the authors outlined the HPTM solution procedure for general nonlinear fractional differential equations) is applied to obtain analytic solutions for the time fractional chemotaxis-haptotaxis model (Equation 1). To this end, the Laplace transform operator is applied to both sides of each fractional equation in (Equation 1) to obtain the following set of equations after simplification.

$$\begin{cases} \mathcal{L}[u(\zeta,\varsigma)] - \dfrac{e^{-\varepsilon\zeta^2}}{s} - \dfrac{1}{s^{\sigma}}\mathcal{L}\left[d_u\dfrac{\partial^2 u}{\partial\zeta^2} - \chi\dfrac{\partial}{\partial\zeta}\left(u\dfrac{\partial v}{\partial\zeta}\right) - \xi\dfrac{\partial}{\partial\zeta}\left(u\dfrac{\partial w}{\partial\zeta}\right) + \mu(1-u-w)\right] = 0, \\ \mathcal{L}[v(\zeta,\varsigma)] - \dfrac{Me^{-\varepsilon\zeta^2}}{s} - \dfrac{1}{s^{\sigma}}\mathcal{L}\left[d_v\dfrac{\partial^2 v}{\partial\zeta^2} - \beta v + \lambda u\right] = 0, \\ \mathcal{L}[w(\zeta,\varsigma)] - \dfrac{1-Me^{-\varepsilon\zeta^2}}{s} - \dfrac{1}{s^{\sigma}}\mathcal{L}[-\delta vw + \eta w(1-w-u)] = 0. \end{cases} \tag{17}$$

Applying the inverse Laplace transform to each expression in (Equation 17) gives:

$$\begin{cases} u(\zeta,\varsigma) = e^{-\varepsilon\zeta^2} + \mathcal{L}^{-1}\left\{\dfrac{1}{s^{\sigma}}\mathcal{L}\left[d_u\dfrac{\partial^2 u}{\partial\zeta^2} - \chi\dfrac{\partial}{\partial\zeta}\left(u\dfrac{\partial v}{\partial\zeta}\right) - \xi\dfrac{\partial}{\partial\zeta}\left(u\dfrac{\partial w}{\partial\zeta}\right) + \mu u(1-u-w)\right]\right\}, \\ v(\zeta,\varsigma) = Me^{-\varepsilon\zeta^2} + \mathcal{L}^{-1}\left\{\dfrac{1}{s^{\sigma}}\mathcal{L}\left[d_v\dfrac{\partial^2 v}{\partial\zeta^2} - \beta v + \alpha u\right]\right\}, \\ w(\zeta,\varsigma) = 1 - Me^{-\varepsilon\zeta^2} + \mathcal{L}^{-1}\left\{\dfrac{1}{s^{\sigma}}\mathcal{L}[-\delta vw + \eta w(1-u-w)]\right\} = 0. \end{cases} \tag{18}$$

With respect to the algorithm for the HPTM solution algorithm, assume that the solution of (Equation 1) can be expressed as power series in the following form:

$$u(\zeta,\varsigma)=\sum_{i=0}^{\infty}p^{i}u_{i}(\zeta,\varsigma)\,,\qquad v(\zeta,\varsigma)=\sum_{i=0}^{\infty}p^{i}v_{i}(\zeta,\varsigma)\,,\qquad w(\zeta,\varsigma)=\sum_{i=0}^{\infty}p^{i}w_{i}(\zeta,\varsigma).$$

Then (Equation 18) becomes:

$$\begin{cases}\displaystyle\sum_{i=0}^{\infty}p^{i}u_{i}(\zeta,\varsigma)=e^{-\varepsilon\zeta^{2}}+p\mathcal{L}^{-1}\left\{\frac{1}{s^{\sigma}}\,\mathcal{L}\left[\begin{array}{l}d_{u}\,\dfrac{\partial^{2}}{\partial\zeta^{2}}\left(\displaystyle\sum_{i=0}^{\infty}p^{i}u_{i}\right)-\chi\displaystyle\sum_{i=0}^{\infty}p^{i}\mathcal{H}_{i}^{1}(u,v,w)\\ -\xi\displaystyle\sum_{i=0}^{\infty}p^{i}\mathcal{H}_{i}^{2}(u,v,w)+\mu\mathcal{H}_{i}^{3}(u,v,w)\end{array}\right]\right\},\\ \displaystyle\sum_{i=0}^{\infty}p^{i}v_{i}(\zeta,\varsigma)=Me^{-\varepsilon\zeta^{2}}+p\mathcal{L}^{-1}\left\{\frac{1}{s^{\sigma}}\,\mathcal{L}\left[d_{v}\,\frac{\partial^{2}}{\partial\zeta^{2}}\left(\sum_{i=0}^{\infty}p^{i}v_{i}\right)-\alpha\sum_{i=0}^{\infty}p^{i}v_{i}+\beta\sum_{i=0}^{\infty}p^{i}v_{i}\right]\right\},\\ \displaystyle\sum_{i=0}^{\infty}p^{i}w_{i}(\zeta,\varsigma)=1-Me^{-\varepsilon\zeta^{2}}+p\mathcal{L}^{-1}\left\{\frac{1}{s^{\sigma}}\,\mathcal{L}\left[-\delta\sum_{i=0}^{\infty}p^{i}\mathcal{H}_{i}^{4}(u,v,w)+\eta\mathcal{H}_{i}^{5}(u,v,w)\right]\right\}.\end{cases}\tag{19}$$

where $\mathcal{H}_{\mathrm{i}}^{1}(\mathrm{u},\mathrm{v},\mathrm{w})$, $\mathcal{H}_{\mathrm{i}}^{2}(\mathrm{u},\mathrm{v},\mathrm{w})$, $\mathcal{H}_{\mathrm{i}}^{3}(\mathrm{u},\mathrm{v},\mathrm{w})$, $\mathcal{H}_{\mathrm{i}}^{4}(\mathrm{u},\mathrm{v},\mathrm{w})$, $\mathcal{H}_{\mathrm{i}}^{5}(\mathrm{u},\mathrm{v},\mathrm{w})$ are He's polynomials for the nonlinear terms of the model. By comparing coefficients with the same exponents of p in (Equation 19), the following relations are obtained:

$$\begin{cases} p^0: \begin{cases} u_0(\zeta,\varsigma) = e^{-\varepsilon\zeta^2} \\ v_0(\zeta,\varsigma) = Me^{-\varepsilon\zeta^2} \\ w_0(\zeta,\varsigma) = 1 - Me^{-\varepsilon\zeta^2} \end{cases} \\ p^1: \begin{cases} u_1(\zeta,\varsigma) = \mathcal{L}^{-1}\left\{\frac{1}{s^{\sigma}}\,\mathcal{L}\left[d_u\,\frac{\partial^2 u_0}{\partial\zeta^2} - \chi\,\mathcal{H}_0^1(u,v,w) - \xi\mathcal{H}_0^2(u,v,w) + \mu\mathcal{H}_0^3(u,v,w)\right]\right\} \\ v_1(\zeta,\varsigma) = \mathcal{L}^{-1}\left\{\frac{1}{s^{\sigma}}\,\mathcal{L}\left[d_v\,\frac{\partial^2 v_0}{\partial\partial\zeta^2} - \beta v_0 + \alpha u_0\right]\right\} \\ w_1(\zeta,\varsigma) = \frac{1}{s^{\sigma}}\,\mathcal{L}[-\delta\mathcal{H}_0^4(u,v,w) + \eta\mathcal{H}_0^5(u,v,w)] \end{cases} \\ p^2: \begin{cases} u_2(\zeta,\varsigma) = \mathcal{L}^{-1}\left\{\frac{1}{s^{\sigma}}\,\mathcal{L}\left[d_u\,\frac{\partial^2 u_0}{\partial\zeta^2} - \chi\,\mathcal{H}_1^1(u,v,w) - \xi\mathcal{H}_1^2(u,v,w) + \mu\mathcal{H}_1^3(u,v,w)\right]\right\} \\ v_2(\zeta,\varsigma) = \mathcal{L}^{-1}\left\{\frac{1}{s^{\sigma}}\,\mathcal{L}\left[d_v\,\frac{\partial^2 v_1}{\partial\zeta^2} - \beta v_1 + \alpha u_1\right]\right\} \\ w_2(\zeta,\varsigma) = \frac{1}{s^{\sigma}}\,\mathcal{L}[-\delta\mathcal{H}_1^4(u,v,w) + \eta\mathcal{H}_1^5(u,v,w)] \end{cases} \\ \qquad\qquad . \\ p^{n+1}: \begin{cases} u_{n+1}(\zeta,\varsigma) = \mathcal{L}^{-1}\left\{\frac{1}{s^{\sigma}}\,\mathcal{L}\left[d_u\,\frac{\partial^2 u_n}{\partial\zeta^2} - \chi\,\mathcal{H}_n^1(u,v,w) - \xi\mathcal{H}_n^2(u,v,w) + \mu\mathcal{H}_n^3(u,v,w)\right]\right\} \\ v_{n+1}(\zeta,\varsigma) = \mathcal{L}^{-1}\left\{\frac{1}{s^{\sigma}}\,\mathcal{L}\left[d_v\,\frac{\partial^2 v_n}{\partial\zeta^2} - \beta v_n + \alpha u_n\right]\right\} \\ w_{n+1}(\zeta,\varsigma) = \frac{1}{s^{\sigma}}\,\mathcal{L}[-\delta\mathcal{H}_n^4(u,v,w) + \eta\mathcal{H}_n^5(u,v,w)]. \end{cases} \end{cases} \tag{20}$$

For the sake of computational simplicity, assume that $\mu = \eta = 0$. Then by using the initial conditions (Equation 2) in (Equation 20) the following few HPTM solution iterations are obtained:

$$\begin{cases} u_0(\zeta,\varsigma) = \mathrm{e}^{-\varepsilon\zeta^2}, \qquad v_0(\zeta,\varsigma) = M\mathrm{e}^{-\varepsilon\zeta^2}, \qquad w_0(\zeta,\varsigma) = 1 - M\mathrm{e}^{-\varepsilon\zeta^2} \\ u_1(\zeta,\varsigma) = \dfrac{\left(2kd_u\left(2\zeta^2k-1\right) - 2Mk\left(4\zeta^2k-1\right)(\chi-\xi)\,\mathrm{e}^{-k\zeta^2}\right)\mathrm{e}^{-k\zeta^2}\varsigma^{\sigma}}{\Gamma(\sigma+1)} \\ v_1(\zeta,\varsigma) = \dfrac{\left(\sigma + M\left(2kd_v\left(2\zeta^2k-1\right) - \beta\right)\right)\mathrm{e}^{-k\zeta^2}\varsigma^{\sigma}}{\Gamma(\sigma+1)} \\ w_1(\zeta,\varsigma) = \dfrac{M\delta\left(M\mathrm{e}^{-k\zeta^2} - 1\right)\mathrm{e}^{-k\zeta^2}\varsigma^{\sigma}}{\Gamma(\sigma+1)} \\ \qquad\qquad . \\ \qquad\qquad . \\ \qquad\qquad . \end{cases} \tag{21}$$

Consequently, all HPTM solution iterations for $n \geq 2$ can be generated from (Equation 20) in the same manner. Finally, the HPTM series solution for the chemotaxis-haptotaxis model (Equations (1 and 2) is given by

$$\begin{cases} u(\zeta,\varsigma) = u_0(\zeta,\varsigma) + u_1(\zeta,\varsigma) + u_2(\zeta,\varsigma) + \cdots \\ v(\zeta,\varsigma) = v_0(\zeta,\varsigma) + v(\zeta,\varsigma) + v(\zeta,\varsigma) + \cdots, \\ w(\zeta,\varsigma) = w_0(\zeta,\varsigma) + w_1(\zeta,\varsigma) + w_2(\zeta,\varsigma) + \cdots \end{cases} \quad (22)$$

Remark: Clearly, by setting $\hbar = -1$ and $n = 1$, the q −HATM solution iteration reduces the HPTM solution iterations for the model Equations 1-2.

3. RESULTS AND DISCUSSION

In this section, numerical simulations are obtained for the time fractional chemotaxis-haptotaxis model (Equation 1). These simulations are compared for different values of the fractional parameter σ using the q-HATM and HPTM iterative schemes in (Equation 14) and (Equation 20), respectively. In this direction, the numerical simulations for the q −HATM solution (Equation 16) and HPTM solution (Equation 22) are compared using the following set of values for the parameters:

$$\beta = 0.5, \alpha = 0.3, \delta = 10, \mathrm{d_u} = 0.001, \mathrm{d_v} = 0.01, \chi = 0.02, \xi = 0.02.$$

Additionally, it is assumed that $\mu = 0,\ \eta = 0$ for the sake of computational simplicity and $M = 0.5, \varepsilon = 100$ in the initial data (Equation 2).

The 2D-plot in Figure 1(a) demonstrates the behaviour of the coupled q-HATM series solutions (Equation 16) at $\sigma = 1,\ \mathrm{n} = 1,\ \hbar = -1$ and $\varsigma = 0$ while the 2D-plot in Figure 1(b) demonstrate the behaviour of the coupled HPTM series solution (Equation 22) at $\sigma = 1$ and $\mathrm{t} = 0$. It can be observed from the curves that at $\varsigma = 0$ the tumor cell density (black line), ECM density (red line) and MDE concentration (blue line) are identical to those obtained in existing literature (Anderson et al., (2000). Using the $\mathrm{u_{q-HATM}}$ and $\mathrm{u_{HPTM}}$ iterative schemes in (Equation 14) and (Equation 20), respectively, the plots in Figure 2 demonstrate the behaviour of the series solutions for the tumor cells at distinct values of the fractional order parameter: $\sigma = 1,\ \sigma = 0.95,\ \sigma = 0.85$, and $\sigma = 0.65$. Figure 2(a) shows the plots for the $\mathrm{u_{q-HATM}}$ series solutions in (Equation 16) at $\varsigma = 0, \mathrm{n} = 1, \hbar = -1$ and Figure 2(b) shows the plots for the $\mathrm{u_{HPTM}}$ series solutions in (Equation 22) at $\varsigma = 0$. Clearly both $\mathrm{u_{q-HATM}}$ and $\mathrm{u_{HPTM}}$ series solutions varies continuously with respect to the fractional order parameter. In Figure 3, the plots compare the behaviour of the series solutions for the ECM density at distinct values of the fractional order parameter: $\sigma = 1,\ \sigma = 0.95,\ \sigma = 0.85$, and $\sigma = 0.65$. Figure 3(a) shows the plots for the $\mathrm{v_{q-HATM}}$ series solutions in (16) at $\varsigma = 0, \mathrm{n} = 1, \hbar = -1$ and Figure 3(b) shows the plots for the $\mathrm{v_{HPTM}}$ series solutions in (22) at $\varsigma = 0$. As in Figure 2, the $\mathrm{v_{q-HATM}}$ and $\mathrm{v_{HPTM}}$ series solutions vary continuously with respect to the fractional order parameter. In Figure 4, the numerical behaviour of the series solutions for the MDE concentration at $\sigma = 1,\ \sigma = 0.95,\ \sigma = 0.85$, and $\sigma = 0.65$ are compared. Figure 4(a) shows the plots for the $\mathrm{w_{q-HATM}}$ series solutions in (16) at $\varsigma = 0, \mathrm{n} = 1, \hbar = -1$ and Figure 4(b) shows the plots for the $\mathrm{w_{HPTM}}$ series solutions in (22) at $\varsigma = 0$. The simulations in Figure 4 show that the $\mathrm{w_{q-HATM}}$ and w_{HPTM} series solutions varies continuously with respect to the fractional order parameter.

Clearly, from each of the plots in Figures 2-4, the memory effect of the system increases until it stabilizes after some time. Clearly, from Figure 2 to Figure 4 clearly demonstrates that as the fractional order parameter decreases from 1 to 0.65, the memory effect of the system increases until it stabilizes after some time. The simulations demonstrated in Figures 2-4 show that complete agreement between both q − HATM and HPTM series solution for the fractional chemotaxis-haptotaxis model is achieved. Thus the methods work efficiently for a wide class of fractional order mathematical models arising in mathematical biology.

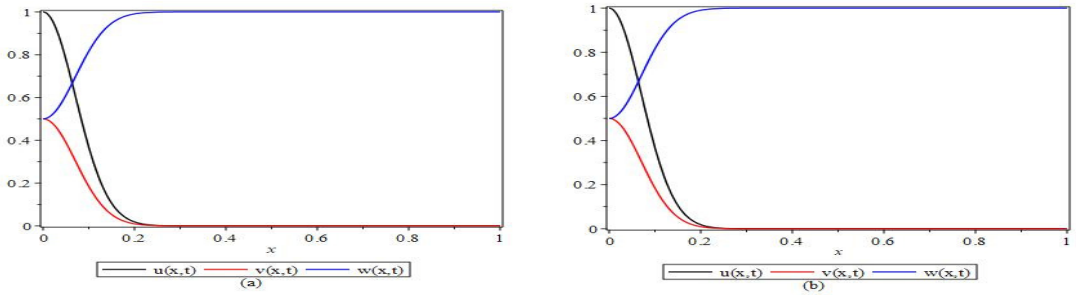

Figure 1: (a) Behaviour of the coupled q-HATM series solutions (16) for the time-fractional chemotaxis-haptotaxis model (Equation 1and 2) at $\varsigma = 0, n = 1, \hbar = -1$ and $\sigma = 1$; (b) Behaviour of the coupled HPTM series solutions (22) for the time-fractional chemotaxis-haptotaxis model (Equation 1and 2) at $\varsigma = 0$ and $\sigma = 1$

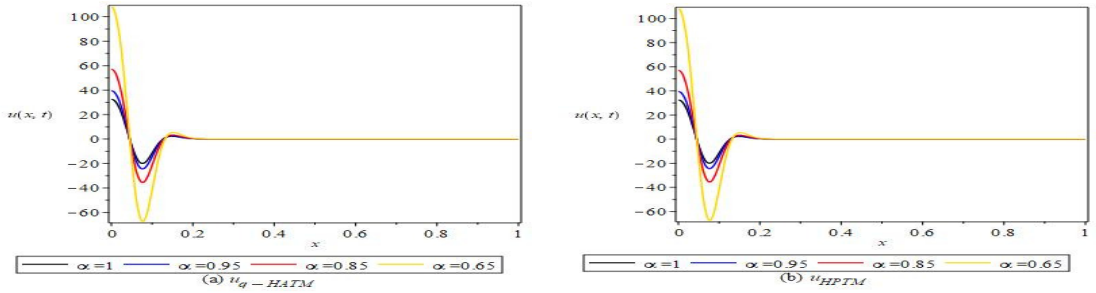

Figure 2: (a) u_{q-HATM} series solutions at $\varsigma = 0, n = 1, \hbar = -1$ and distinct values of σ (b) u_{HPTM} series solutions at $\varsigma = 0$ and distinct values of σ

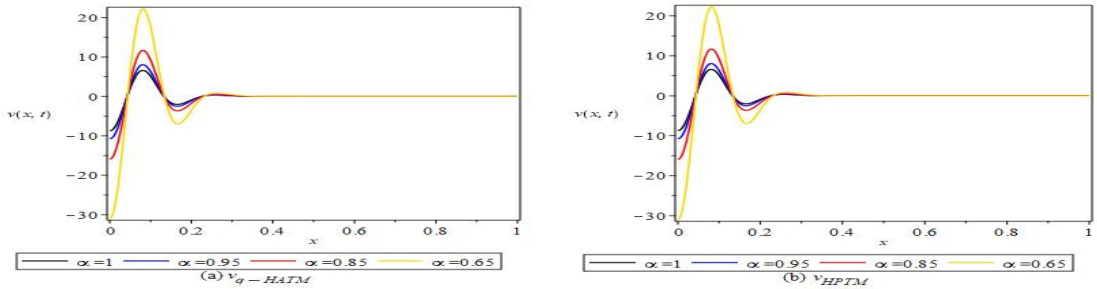

Figure 3: (a) v_{q-HATM} series solutions at $\varsigma = 0, n = 1, \hbar = -1$ and distinct values of σ (b) v_{HPTM} series solutions at $\varsigma = 0$ and distinct values of σ

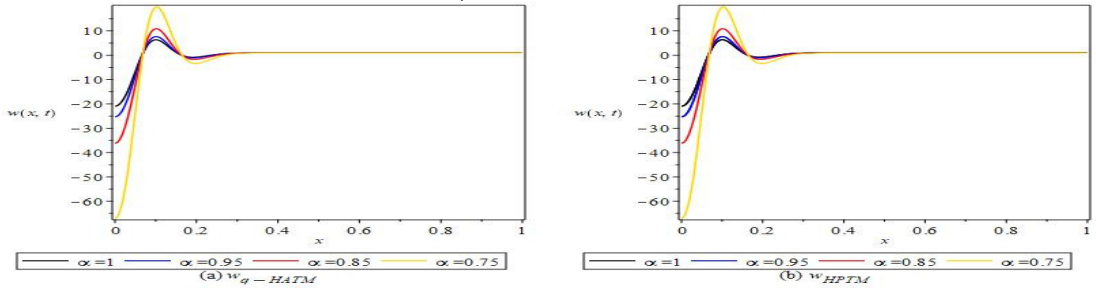

Figure 4: (a) w_{q-HATM} series solutions at $\varsigma = 0, n = 1, \hbar = -1$ and distinct values of σ (b) w_{HPTM} series solutions at $\varsigma = 0$ and distinct values of σ

4. CONCLUSION

In this paper, q-HATM and HPTM were successfully applied to obtain approximate analytic solutions for a time fractional chemotaxis-haptotaxis model. The q-HATM provides an asymptotic parameter $\hbar$ which helps to control the convergence region of the approximate series solution. This is a fundamental qualitative difference in comparison with other similar methods. Apart from being straight forward, both methods do not involve any form of linearization or discretization and are free from any of restrictive assumption. They also provide more realistic series solutions with fast convergence rate. From the obtained numerical results as well as graphical plots, it suffices to say that both the q-HATM and HPTM work efficiently for the time fractional chemotaxis-haptotaxis model and can be effectively employed to examine a wide class of nonlinear mathematical models with fractional derivatives describing even more complex physical phenomena.

5. ACKNOWLEDGMENT

The authors wish to thank the reviewers for their constructive comments and suggestions that have helped us to improve the manuscript significantly.

6. CONFLICT OF INTEREST

There is no conflict of interest associated with this work.

REFERENCES

Adomian G. (1988). A review of the decomposition method in applied mathematics. *Journal of Mathematical Analysis and Applications*, 135, pp. 501–544.

Anderson A. R. A. and Chaplain M. A. J., Newman E. L., Steele R. J. C. and Thompson A. M. (2000). Mathematical modelling of tumor invasion and metastasis. *Journal of Theoretical Medicine*, 2, pp. 129-154.

Berry H. and Larreta-Garde V. (1999). Oscillatory Behaviour of a Simple Kinetic Model for Proteolysis during Cell Invasion. *Biophysical Journal*, 77, pp. 655-665.

Chaplain M.A.J. and Lolas G. (2006). Mathematical modelling of cancer invasion of tissue: dynamic heterogeneity. *Networks and Heterogeneous Media*, 1, pp. 399-439.

El-Tawil, M. A. and Huseen, S. N. (2012). The q −Homotopy Analysis Method (q-HAM). *International Journal of Applied Mathematics and Mechanics,* 8, pp. 51 -75.

Gatenby, R. A. and Gawlinski, E. T. (1996). A reaction-diffusion model for cancer invasion. *Cancer Research*, 56, pp. 5745-5753

He J. H. (1998). An approximate solution technique depending on an artificial parameter: a special example. *Communications in Nonlinear Science and Numerical Simulation*, 3, pp. 92-97

He, J. H. (1997). Variational iteration method for delay differential equations. *Communications in Nonlinear Science and Numerical Simulation*, 2, pp. 235-236.

He, J. H. (1999). Homotopy perturbation technique. *Computer Methods in Applied Mechanics and Engineering,* 178, pp. 257–262

He, J. H. (2003). Homotopy perturbation method: a new nonlinear analytical technique. *Applied Mathematics and Computation,* 135, pp. 73–79

He, J. H. (2006). New interpretation of homotopy perturbation method. *International Journal of Modern Physics B*, 20, pp. 2561–2568

Khan, Y. and Wu, Q. (2011). Homotopy perturbation transform method for nonlinear equations using He's polynomials. *Computers and Mathematics with Applications,* 61, pp. 1963–1967.

Kilbas, A. A., Srivastava, H. M. and Trujillo, J. J. (2006). *Theory and applications of fractional differential equations*. Elsevier, Amsterdam.

Liao, S. J. (1992). *The proposed homotopy analysis technique for the solution of nonlinear problems*. Ph.D. Thesis: Shanghai Jiao Tong University.

Liao, S. J. (1997). Homotopy analysis method and its applications in mathematics. *Journal of Basic Science* and *Engineering*. 5, pp. 111-125.

Lin B., Holmes W. R., Wang C. J., Ueno T., Harwell A., Edelstein-Keshet L., Inoure T. and Levchenko A. (2012). Synthetic Spatially Graded Rac Activation Drives Cell Polarization and Movement, PNAS, E3668-E3667.

Markl, C., Meral, G. and Surulescu, C. (2013). Mathematical analysis and numerical simulation for a system modeling acid-mediated tumor cell invasion. *International Journal of Analysis*. Article ID 878051, 15 pages.

McAneney H. and O Rourke S.F.C. (2007). Investigation of Various Growth Mechanisms of Solid Tumour Growth within the Linear-Quadratic Model for Radiotherapy. *Physics in Medicine and Biology*, 52, pp. 1039-1054.

Newton I. O. and Abel M. J. (2020). Application of the $\boldsymbol{q}$−homotopy analysis transform method ($\boldsymbol{q}$−HATM) to the solution of a fractional attraction Keller-Segel chemotaxis model. *Science World Journal,* 15, pp. 1-12

Podlubny, I. (1999) *Fractional Differential Equations*. Academic, New York.

Prakash, A. and Kumar, M. (2016a), He's variational iteration method for the solution of nonlinear Newell-Whitehead-Segel equation. *Journal of Applied Analysis and Computation*, 6, pp. 738-748.

Prakash, A. and Kumar, M. (2016b), Numerical solution of two dimensional time fractional-order biological population model. *Open Physics*, 14, pp. 177-186.

Prakash, A., Kumar, M. and Sharma, K.K. (2015), Numerical method for solving fractional coupled Burgers equations. *Applied Mathematics and Computation*, 260, pp. 314-320.

Prakash, A., Veeresha, P., Prakasha, D. G. and Goyal, M. A. (2019). New efficient technique for solving fractional coupled Navier–Stokes equations using q-homotopy analysis transform method. *Pramana – Journal of Physics,* 93, Article ID 0006.

Sachs R. K., Hlatky L. R. and Hahnfeldt P. (2001). Simple ODE Models of Tumor Growth and Anti-Angiogenic or Radiation Treatment. *Mathematical and Computer Modelling*, 33, pp. 1297-1305.

Singh, J., Kumar, D. and Swroop, R. (2016). Numerical solution of time and space-fractional coupled Burgers' equations via homotopy algorithm. *Alexandria Engineering Journal*, 55, pp. 1753–1763.

Tiwana, M.H., Maqbool, K. and Mann. A. B. (2017). Homotopy perturbation Laplace transform solution of fractional non-linear reaction diffusion system of Lotka-Volterra type differential equation. *Engineering Science and Technology, an International Journal,* 20, pp. 672–678

Veeresha, P., Prakasha, D. G., Qurashi, M. A. and Baleanu, D. A. (2019). Reliable technique for fractional modified Boussinesq and approximate long wave equations. *Advances in Difference Equations,* 253.

Wazwaz A. M. and El-Sayed S. M. (2001). A new modification of the Adomian decomposition method for linear and nonlinear operators. *Applied Mathematics and Computation*, 122, pp. 393–405.

Yildirim, A. (2009). An algorithm for solving the fractional nonlinear Schrödinger equation by means of the homotopy perturbation method. *International Journal of Nonlinear Sciences and Numerical Simulation*, 10, pp. 445-450.

Yildirim, A. (2010). Analytical approach to Fokker-planck equation with space- and time- fractional derivatives by means of the homotopy perturbation method. *Journal of King Saud University (Science)*, 22, pp. 257-264.